Frequency-Load Interaction of Imperfect Angle-Ply Cylindrical Panels Under Compression and Pressure

Isaac Du* and David Hui†
The Ohio State University, Columbus, Ohio

This paper deals with the influence of geometric imperfections on the linear vibration frequencies of thin, laminated angle-ply, simply supported antisymmetric cylindrical panels under axial compression and lateral pressure. It is found that the presence of small geometric imperfections of the order of a fraction of the shell thickness may significantly raise the fundamental frequencies and change the optimal fiber angle that maximizes the frequency. The interaction curves between frequency axial load and frequency-pressure are plotted for graphite-epoxy angle-ply cylindrical panels likely to be encountered in practice.

Nomenclature

Dimensional Quantities

$[A^*]$ $= [A]^{-1}$
$[B^*]$ $= -[A]^{-1}[B]$
$[D^*]$ $= [D] - [B][A]^{-1}[B]$
$[A],[B],[D]$ = matrices describing material constitutive relations
B = curved distance between two longitudinal edges
E_1, E_2 = Young's moduli in the direction of the fiber and transverse to the fiber, respectively
F = stress function
G_{12} = shear modulus of an orthotropic layer
h = total thickness of laminated shell
L = length of cylindrical panel
$L_A^*(\ )$ $= A_{22}^*(\ )_{,XXXX} + (2A_{12}^* + A_{66}^*(\ )_{,XXYY} + A_{11}^*(\ )_{,YYYY}$
$L_B^*(\ )$ $= (2B_{26}^* - B_{61}^*)(\ )_{,XXXY} + (2B_{16}^* - B_{62}^*)(\ )_{,XYYY}$
$L_D^*(\ )$ $= D_{11}^*(\ )_{,XXXX} + 2(D_{12}^* + 2D_{66}^*)(\ )_{,XXYY} + D_{22}^*(\ )_{,YYYY}$
N_x, N_y = membrane stress resultants
$\bar{p}$ = lateral pressure (positive for external pressure)
$\bar{p}_c$ = buckling load due to external lateral pressure
R = shell radius
$\bar{t}$ = time
U, V = axial and circumferential displacements, respectively
W = out-of-plane displacement
W_0 = initial geometric imperfection
X, Y = axial and circumferential coordinates, respectively
ρ = mass of shell per unit surface area
$\bar{\omega}$ = frequency
ω_r = reference frequency

Nondimensional Quantities

$[a^*],[b^*],[d^*]$ $= [A^*]E_2h,\ [B^*]/h,\ [D^*]/(E_2h^3)$
$C_a^*(P,Q)$ $= a_{22}^*P^4 + (2a_{12}^* + a_{66}^*)P^2Q^2 + a_{11}^*Q^4$
$C_b^*(P,Q)$ $= (2b_{26}^* - b_{61}^*)P^3Q + (2b_{16}^* - b_{62}^*)PQ^3$
c_w = amplitude of the previbration diplacement
f $= F/(E_2h^3)$
f_B = stress function in vibration state
f_p = stress function in previbration static state
j = number of axial half-waves in the geometric imperfection and previbration displacement
J $= j\pi B/(L\theta_s)$
k = the number of circumferential half-waves in the geometric imperfection and previbration displacement
K $= k\pi/\theta_s$
$L_{a^*}(\ )$ $= a_{22}^*(\ )_{,xxxx} + (2a_{12}^* + a_{66}^*)(\ )_{,xxyy} + a_{11}^*(\ )_{,yyyy}$
$L_{b^*}(\ )$ $= (2b_{26}^* - b_{61}^*)(\ )_{,xxxy} + (2b_{16}^* - b_{62}^*)(\ )_{,xyyy}$
$L_{d^*}(\ )$ $= d_{11}^*(\ )_{,xxxx} + 2(d_{12}^* + 2d_{66}^*)(\ )_{,xxyy} + d_{22}^*(\ )_{,yyyy}$
ℓ $= B/(L\theta_s^2)$
m = number of axial half-waves in the vibration mode
M $= m\pi B/(L\theta_s)$
n = number of circumferential half-waves in the vibration mode
N $= n\pi/\theta_s$
N_L = number of layers
p $= \bar{p}R^2/(E_2h^2)$
t $= \omega_r\bar{t}$; nondimensional time
(w, w_0) $= (W/h, W_0/h)$
w_B = out-of-plane vibration displacement
w_p = previbration static out-of-plane displacement
(x,y) $= (X,Y)/(Rh)^{1/2}$
θ_s $= B/(Rh)^{1/2}$; the simplified-flatness parameter
μ = amplitude of the imperfection normalized with respect to the total thickness of the laminated shell
ν_{12} = Poisson's ratio
σ_x $= N_xR/(E_2h^2)$
ω $= \bar{\omega}/\omega_r$; nondimensional frequency
ω^* $= (\theta_s)^2\omega$ for $\theta_s < 1$ and $\omega^* = \omega$ for $\theta_s > 1$

I. Introduction

THE influence of geometric imperfections on vibration of isotropic homogeneous plates and shells has been a subject of considerable interest over the past ten years. The effects of imperfections on vibrations of rectangular plates,[1-3] open cylindrical panels,[4] closed cylindrical shells,[5-8] and spherical shells[9] have been examined.

Received Feb. 13, 1986; revision received July 22, 1986. Copyright © American Institute of Aeronautics and Astronautics, Inc., 1986. All rights reserved.

*Doctoral Student, Department of Engineering Mechanics.
†Assistant Professor, Department of Engineering Mechanics. Member AIAA.

The effects of these imperfections on vibrations of composite (laminated) rectangular plates have also been studied. Such effects on vibration of laminated antisymmetric angle- and cross-ply rectangular plates with various in-plane and out-of-plane boundary conditions were investigated by Hui[10,11] and verified using the finite-element method by Kapania and Yang.[12] Further work on the vibration of symmetrically laminated, imperfect rectangular plates with rotationally restrained edges was conducted by Bhattacharya.[13] However, it appears that the present paper is the first attempt in the open literature to study the effects of imperfections on vibration of composite-material shells.

The present investigation deals with the effects of geometric imperfections on the linear fundamental frequencies of simply supported, antisymmetric laminated angle-ply cylindrical panels under axial compression and internal and external lateral pressure. From previous studies, the presence of an imperfection of the same spatial form as the vibration mode will significantly increase (with some exceptions) the vibration frequencies of plates and shells, even for imperfection amplitude of the order of a fraction of the thickness. This demonstrates that the actual geometric imperfection of arbitrary shape encountered in practice cannot be "safely" neglected. In addition to the complicated effects of the geometric and material parameters, the present study aims to emphasize the interactions between the geometric imperfections, the preloads, and their effects on the optimum fiber angle that maximizes the fundamental frequency in typical vibration problems. Certain trends in the vibration frequencies of laminated cylindrical panels that cannot be deduced from the laminated rectangular plates are noted and discussed.

The analysis is based on a solution of Donnell-type nonlinear equilibrium and compatibility equations of a laminated cylindrical shell. The previbration, static nonlinear compatibility equation is satisfied exactly, and the static nonlinear previbration equilibrium is solved approximately using a Galerkin procedure. Similarly, the linearized dynamic compatibility equation is satisfied exactly, and the linearized dynamic equilibrium is solved approximately using a Galerkin method. Thus, despite the one-term solution used in the present analysis, the computed frequencies are upper bounds. An explicit relation involving the vibration frequency, the axial compression, and lateral pressure preloads is obtained in closed form in terms of the wavenumbers of the geometric imperfections and the vibration mode. The fundamental frequency is searched for all possible discrete values of the vibration wavenumbers.

Example problems are chosen from various angle-ply, simply supported, square cylindrical panels that may be encountered in practice. Frequency-axial load and frequency-pressure interaction curves are plotted for perfect and imperfect antisymmetric angle-ply cylindrical panels.

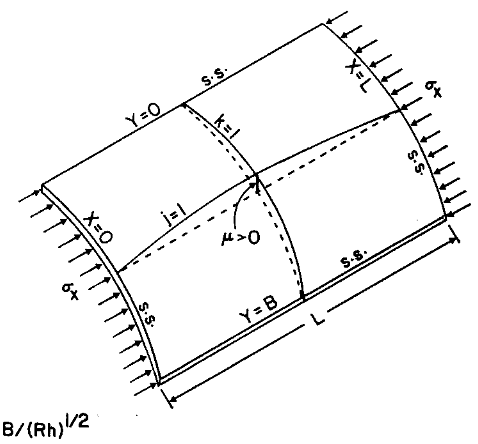

Fig. 1 Geometry of the imperfect laminated cylindrical panels.

II. Governing Differential Equations and Previbration State

The nonlinear equilibrium and compatibility equations of a laminated cylindrical panel, written in terms of an out-of-plane displacement W and a stress function F, incorporating the possibility of the presence of an initial geometric imperfection W_0, are, respectively,[14,15]

$$\begin{aligned} &\rho W,_{\bar t\bar t} + L_{D^*}(W) + L_{B^*}(F) + (1/R)F,_{XX} \\ &= F,_{YY}(W+W_0),_{XX} + F,_{XX}(W+W_0),_{YY} \\ &-2F,_{XY}(W+W_0),_{XY} - \bar p \end{aligned} \tag{1}$$

$$\begin{aligned} &L_{A^*}(F) = L_{B^*}(W) + [(W+W_0),_{XY}]^2 - (W_{0,XY})^2 \\ &+(1/R)(W,_{XX}) - (W+W_0),_{XX}(W+W_0),_{YY} \\ &+ W_{0,XX}W_{0,YY} \end{aligned} \tag{2}$$

where X and Y are the axial and circumferential coordinates, R is the shell radius, ρ is the mass of the shell per unit surface area, $\bar p$ is the lateral pressure (positive for external pressure), $\bar t$ is time, and L_{A^*}, L_{B^*}, and L_{D^*} are the differential operators defined by Tennyson et al.[16] Note that W and W_0 are positive outwards. The following nondimensional quantities are introduced:

$$\begin{aligned} &(w,w_0) = (W/h, W_0/h), \quad f = F/(E_2h^3), \quad p = \bar pR^2/(E_2h^2) \\ &(x,y) = (X,Y)/(Rh)^{1/2}, \quad t = \omega_r\bar t, \quad (\omega_r)^2 = E_2h/(\rho R^2) \end{aligned} \tag{3}$$

where h is the total thickness of the laminated shell, ω_r is the reference frequency, and E_2 is Young's modulus in the transverse direction. Thus, the nonlinear equilibrium and compatibility equations, written in the nondimensional form, are, respectively,

$$\begin{aligned} &w,_{tt} + L_{d^*}(W) + L_{b^*}(f) + f,_{xx} = f,_{yy}(w+w_0),_{xx} \\ &+f,_{xx}(w+w_0),_{yy} - 2f,_{xy}(w+w_0),_{xy} - p \end{aligned} \tag{4}$$

$$\begin{aligned} &L_{a^*}(f) = w,_{xx} + L_{b^*}(w) + [(w+w_0),_{xy}]^2 - (w_{0,xy})^2 \\ &-(w+w_0),_{xx}(w+w_0),_{yy} + w_{0,xx}w_{0,yy} \end{aligned} \tag{5}$$

For an angle-ply cylindrical panel, the nondimensional linear operators are

$$\begin{aligned} &L_{a^*}(\ ) = a^*_{22}(\ ),_{xxxx} + (2a^*_{12} + a^*_{66})(\ ),_{xxyy} + a^*_{11}(\ ),_{yyyy} \\ &L_{b^*}(\ ) = (2b^*_{26} - b^*_{61})(\ ),_{xxxy} + (2b^*_{16} - b^*_{62})(\ ),_{xyyy} \\ &L_{d^*}(\ ) = d^*_{11}(\ ),_{xxxx} + (2)(d^*_{12} + 2d^*_{66})(\ ),_{xxyy} + d^*_{22}(\ ),_{yyyy} \end{aligned} \tag{6}$$

where

$$(a^*_{ij}, b^*_{ij}, d^*_{ij}) = (E_2hA^*_{ij}, B^*_{ij}/h, D^*_{ij}/(E_2h^3)) \tag{7}$$

The laminated cylindrical panel is simply supported at all four edges. The geometric imperfection and the previbration static deflection are assumed to be of the same spatial form

$$[w_p(x,y), w_0(x,y)] = (c_w, \mu)\sin(Jx)\sin(Ky) \tag{8a}$$

where

$$J = j\pi B/(L\theta_s) \qquad K = k\pi/\theta_s \qquad \theta_s = B/(Rh)^{1/2} \tag{8b}$$

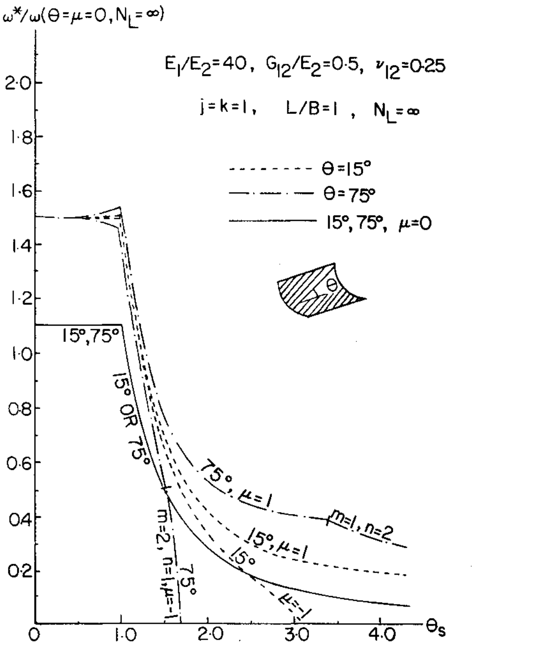

Fig. 2a Fundamental frequency vs simplified-flatness parameter for imperfect, angle-ply (N_L = infinite), simply supported, square cylindrical panels with fiber angle $\theta = 15$ and 75 deg.

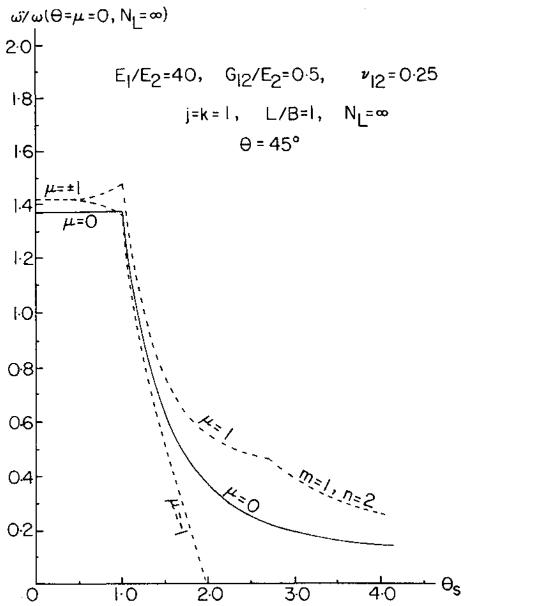

Fig. 2b Fundamental frequency vs simplified-flatness parameter for imperfect, angle-ply (N_L = infinite), simply supported, square cylindrical panels with fiber angle $\theta = 45$ deg.

Although the imperfection shapes are random in practical shell structures, the introduction of geometric imperfections of specified shape will considerably simplify the theoretical analysis, and will provide useful information on the possible effects in a preliminary design, especially if the effects of these imperfections on the vibration behavior are significant. As shown in Fig. 1, L is the length of the cylindrical panel, B is the curved distance between the two longitudinal edges, the positive integers j and k are the number of axial and circumferential half-waves, respectively, and μ is the amplitude of the imperfection normalized with respect to the total thickness of the laminated shell h. Furthermore, the simplified-flatness parameter θ_s is defined to be the ratio of panel width B to the characteristic length $(Rh)^{1/2}$, such that the present problem does not depend on the individual values of R/h and B/R but on $B/(Rh)^{1/2}$.

Substituting $w_0(x,y)$ and $w_p(x,y)$ into the nonlinear compatibility equation of a laminated cylindrical panel, the previbration stress function is found to be[17]

$$f_p(x,y) = f^*(x,y) - (\sigma_x)(y^2/2) - (p)(x^2/2) \tag{9}$$

where,

$$f^*(x,y) = c_0 \sin(Jx)\sin(Ky) + c_f \cos(Jx)\cos(Ky) + [(c_w+\mu)^2 - \mu^2][A_1\cos(2Jx) + A_2\cos(2Ky)] \tag{10}$$

This stress function satisfies the following in-plane boundary conditions approximately[18]:

$$N_y(y=0) = N_y(y=\theta_s) = 0, \quad U(y=0) = U(y=\theta_s) = \text{const}$$
$$N_x(x=0) = N_x(x=L/(Rh)^{1/2}) = 0$$
$$V(x=0) = V(x=L/(Rh)^{1/2}) = \text{const} \tag{11}$$

where the nondimensional axial load σ_x (positive for compression) is defined in terms of the membrane axial stress resultant to be

$$\sigma_x = N_x R/(E_2 h^2) \tag{12}$$

and the remaining coefficients are found to be ($c_0 = -\bar{c}_0 c_w$)

$$c_0 = -J^2 c_w / C_{a^*}(J,K) \qquad c_f = -C_{b^*}(J,K)c_w/C_{a^*}(J,K)$$
$$A_1 = K^2/(32J^2 a_{22}^*) \qquad A_2 = J^2/(32K^2 a_{11}^*) \tag{13}$$

where

$$C_{a^*}(P,Q) = a_{22}^* P^4 + (2a_{12}^* + a_{66}^*)(P^2Q^2) + a_{11}^* Q^4$$
$$C_{b^*}(P,Q) = (2b_{26}^* - b_{61}^*)(P^3Q) + (2b_{16}^* - b_{62}^*)(PQ^3) \tag{14}$$

Finally, substituting $w_0(x,y)$, $w_p(x,y)$, and $f_p(x,y)$ into the nonlinear equilibrium equation and performing the Galerkin procedure, with respect to $\sin(Jx)\sin(Ky)$, one obtains a cubic equation in $c_w + \mu$ in the form

$$(c_w+\mu)^3(A_1+A_2)(J^2K^2/2) + (c_w+\mu)^2\{[16A_1 J\ell/(3K)] + (8JK\bar{c}_0\ell/3)\} + (c_w+\mu)\{(C^*/4) - (8\mu JK\bar{c}_0\ell/3) + (\bar{c}_0 J^2/4) - (A_1+A_2)(\mu^2 J^2K^2/2) - [(J^2\sigma_x + K^2 p)/4]\} - (\mu)[(C^* + J^2\bar{c}_0)/4] - [16\mu^2 A_1 J\ell/(3K)] = 0 \tag{15}$$

where $\ell = B/(L\theta_s^2)$ if both j and k are odd integers, and $\ell = 0$ otherwise. As a check on the analysis, it can be seen that in the special case of zero preload, $\sigma_x = 0$, $p = 0$, the previbration static deflection is identically zero (that is, $c_w = 0$, $c_0 = 0$) for all values of the geometric imperfection amplitudes.

III. Vibration of Laminated Cylindrical Panels with Preload

Using a perturbation technique, the total displacement and stress function can be expressed as the sum of the previbration state and the perturbed state. Substituting $w = w_p(x,y) + w_B(x,y,t)$ and $f = f_p(x,y) + f_B(x,y,t)$ into the nonlinear equilibrium and compatibility equations and linearizing the resulting equations with respect to w_B and f_B, one obtains, respectively

$$w_{,tt} + L_{d^*}(w_B) + L_{b^*}(f_B) + f_{B,xx} + \sigma_x w_{B,xx} + p w_{B,yy}$$
$$= f^*_{,yy} w_{B,xx} + f^*_{,xx} w_{B,yy} - 2f^*_{,xy} w_{B,xy} + (w_p + w_0)_{,xx} f_{B,yy}$$
$$+ (w_p + w_0)_{,yy} f_{B,xx} - 2(w_p + w_0)_{,xy} f_{B,xy} \qquad (16)$$

$$L_{a^*}(f_B) = w_{B,xx} + L_{b^*}(w_B) + (2)(w_p + w_0)_{,xy} w_{B,xy}$$
$$- (w_p + w_0)_{,xx} w_{B,yy} - (w_p + w_0)_{,yy} w_{B,xx} \qquad (17)$$

Using a one-term approximation, the vibration mode that satisfies the simply supported boundary conditions can be expressed in the form

$$w_B(x,y,t) = \sin(Mx)\sin(Ny)\exp(i\omega t) \qquad (18)$$

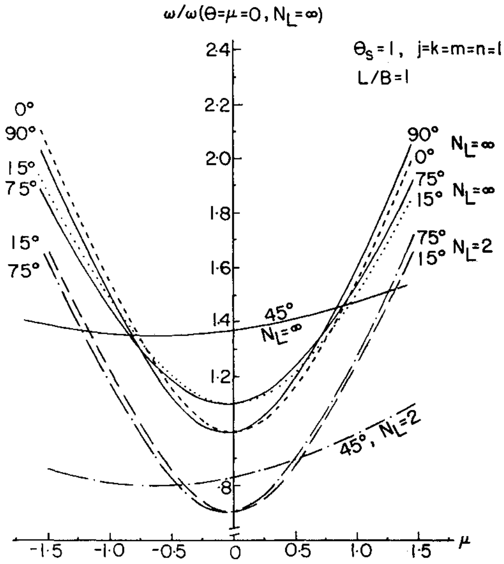

Fig. 3a Fundamental frequency vs imperfection amplitude for angle-ply, simply supported, square cylindrical panels with $\theta_s = 1$ and fiber angle $\theta = (0$ and 90 deg), (15 and 75 deg), and 45 deg.

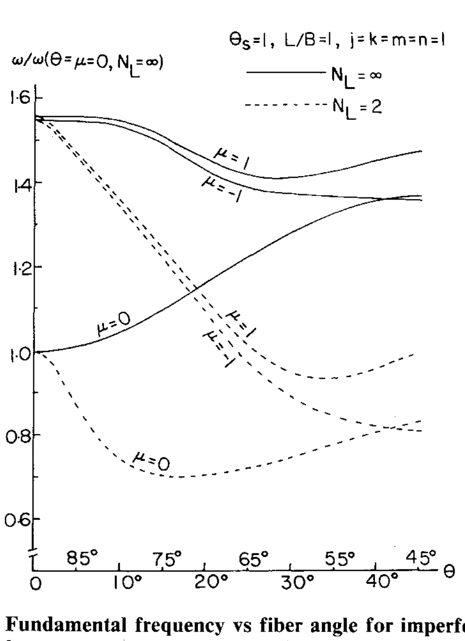

Fig. 3b Fundamental frequency vs fiber angle for imperfect angle-ply, simply supported, square cylindrical panels with simplified-flatness parameter $\theta_s = 1$.

where $i = (-1)^{1/2}$ and $\omega = \bar{\omega}/\omega_r$ where $\bar{\omega}$ is the dimensional frequency. Substituting $w_0(x,y)$, $w_p(x,y)$, and $w_B(x,y,t)$ into the linearized dynamic compatibility equilibrium equation, the stress function that satisfies this equation exactly is found to be

$$f_B(x,y,t) = \{c_1^* \sin(Mx)\sin(Ny) + c_1\cos(Mx)\cos(Ny)$$
$$+ (c_w + \mu)(c_2\cos[(K-N)y] + c_3\cos[(K+N)y])$$
$$\times\cos[(J-M)x] + (c_w + \mu)(c_4\cos[(K-N)y]$$
$$+ c_5\cos[(K+N)y])\cos[(J+M)x]\}\exp(i\omega t) \qquad (19)$$

where

$$c_1^* = -M^2/C_{a^*}(M,N), \quad c_1 = -C_{b^*}(M,N)/C_{a^*}(M,N)$$
$$c_2 = (-1/4)(JN-KM)^2/C_{a^*}(J-M,K-N)$$
$$c_3 = (1/4)(JN+KM)^2/C_{a^*}(J-M,K+N)$$
$$c_4 = (1/4)(JN+KM)^2/C_{a^*}(J+M,K-N)$$
$$c_5 = (-1/4)(JN-KM)^2/C_{a^*}(J+M,K+N) \qquad (20)$$

Finally, substituting $w_0(x,y)$, $w_p(x,y)$, $f^*(x,y)$, $w_B(x,y,t)$, and $f_B(x,y,t)$ into the linearized dynamic equilibrium equation and applying the Galerkin procedure with respect to $\sin(Mx)\sin(Ny)$ where

$$M = m\pi B/(L\theta_s) \qquad N = n\pi/\theta_s \qquad (21)$$

and m is the number of axial half-waves and n the number of circumferential half-waves, one obtains an explicit relation among the frequency ω, the applied axial load σ_x, and the lateral pressure p in the form

$$\omega^2 + \sigma_x M^2 + pN^2 = C_{d^*}(M,N) + [C_{b^*}(M,N)^2/C_{a^*}(M,N)]$$
$$- c_1^* M^2 - 4(c_w + \mu)[C_{b^*}(J-M,K-N)c_2 I_0 H_0$$
$$+ (J-M)^2(c_2 I_0^* H_0^* + c_3 I_0^* H_0^{**})$$
$$+ (J+M)^2(c_4 I_0^{**} H_0^* + c_5 I_0^{**} H_0^{**})]$$
$$- 4(K^2M^2 + J^2N^2)(c_f I_2 H_2 + c_0 I_2^* H_2^*)$$
$$- (8)[(c_w + \mu)^2 - \mu^2](M^2K^2A_2H_1 + J^2N^2A_1I_1)$$
$$+ (8)(JKMN)(c_f I_3 H_3 + c_0 I_3^* H_3^*)$$
$$- (4)(c_w + \mu)(J^2N^2 + K^2M^2)(c_1^* I_2^* H_2^* + c_1 I_3 H_3)$$
$$- (4)(c_w + \mu)^2\{[J^2(K-N)^2 + K^2(J-M)^2](c_2 I_4 H_4)$$
$$+ [J^2(K+N)^2 + K^2(J-M)^2](c_3 I_4 H_5)$$
$$+ [J^2(K-N)^2 + K^2(J+M)^2](c_4 I_5 H_4)$$
$$+ [J^2(K+N)^2 + K^2(J+M)^2](c_5 I_5 H_5)\}$$
$$+ (8)(c_w + \mu)\{(JKMN)(c_1^* I_3^* H_3^* + c_1 I_2 H_2)$$
$$+ (JK)(J-M)[c_2(K-N)I_6H_6 + c_3(K+N)(I_6H_7)]$$
$$+ (JK)(J+M)[c_4(K-N)I_7H_6 + c_5(K+N)(I_7H_7)]\}$$
$$(22)$$

where I_0–I_7 and $H_0, H_1, \ldots, H_7$ are defined[10] by deleting the factor π and replacing k and n with K and N, respectively.

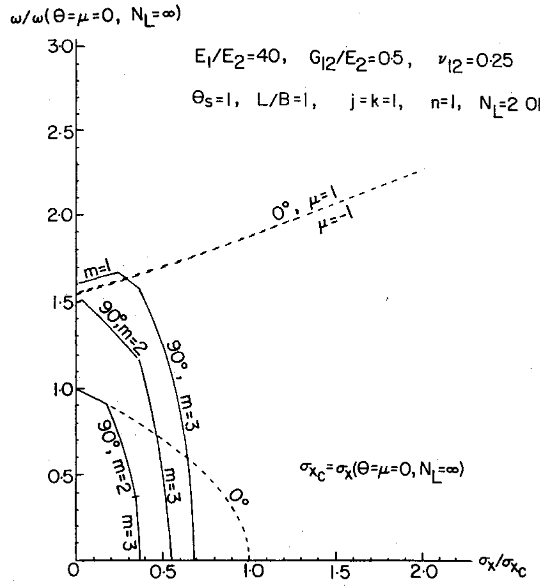

Fig. 4a Fundamental frequency vs normalized uniaxial preload for imperfect angle-ply, simply supported, square cylindrical panels with $\theta_s = 1$ and fiber angle $\theta = 0$ and 90 deg.

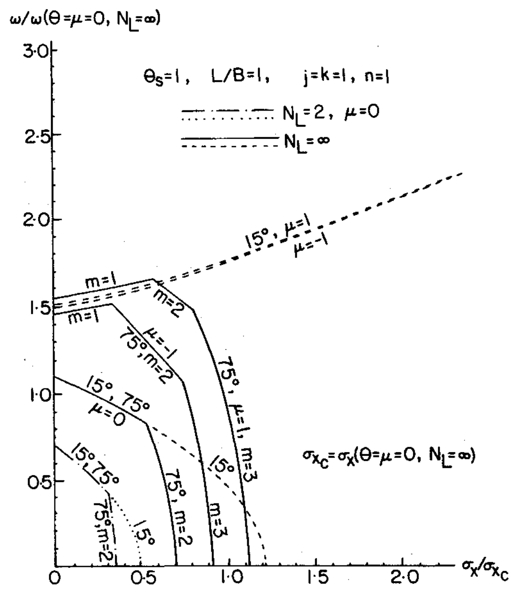

Fig. 4b Fundamental frequency vs normalized uniaxial preload for imperfect angle-ply, simply supported, square cylindrical panels with $\theta_s = 1$ and fiber angle $\theta = 15$ and 75 deg.

Furthermore, I_0^*, I_0^{**}, I_2^*, and I_3^* are defined as

$$I_0^* = [1/(2M-J)] + (1/J)$$

$$I_0^{**} = [1/(2M+J)] - (1/J)$$

$$I_2^* = (1/J) - (1/2)[1/(2M+J)] + (1/2)[1/(2M-J)]$$

$$I_3^* = (1/2)[1/(2M-J)] + (1/2)[1/(2M+J)] \tag{23}$$

with j being an odd integer, and $I_0^* = I_0^{**} = I_2^* = I_3^* = 0$ if j is an even integer. Finally, H_0^*, H_0^{**}, H_2^* and H_3^* can be obtained from I_0^*, I_0^{**}, I_2^*, and I_3^*, respectively, by replacing M with N, J with K, and j with k.

IV. Discussion of Results

The present paper deals with vibration of antisymmetric angle-ply, simply supported cylindrical panels. The geometric

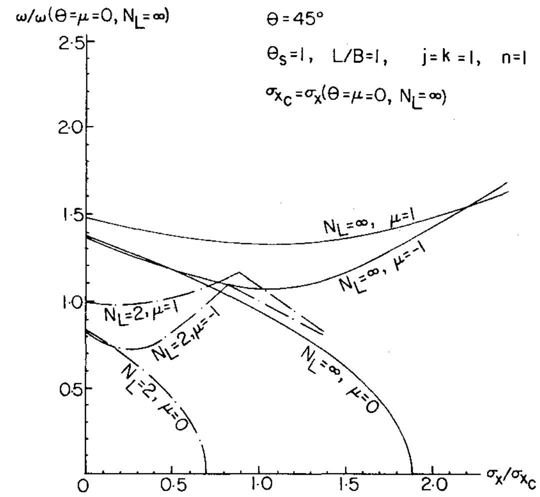

Fig. 4c Fundamental frequency vs normalized uniaxial preload for imperfect angle-ply, simply supported, square cylindrical panels with $\theta_s = 1$ and fiber angle $\theta = 45$ deg.

parameters involve the simplified flatness parameter and the length-to-width ratio. In all the following example problems, the imperfection wavenumbers are chosen to be $j = k = 1$ and the aspect ratio is L/B. Furthermore, each layer is orthotropic and is made to graphite-epoxy material specified by

$$E_1/E_2 = 40 \qquad G_{12}/E_2 = 0.5 \qquad \nu_{12} = 0.25 \tag{24}$$

where G_{12} is the shear modulus and ν_{12} is Poisson's ratio. The number of layers N_L is either two or infinite. Unless otherwise specified, the fundamental vibration mode corresponds to the wavenumbers $m = n = 1$. The frequency for $\theta = \mu = 0$, N_L = infinite is used as the normalizing factor and it is found to be

$$\bar{\omega}(\theta = \sigma = 0, N_L = \text{infinite}) = 18.805[E_2 h/(\rho R^2)]^{1/2} \tag{25}$$

Figure 2a shows a graph of the fundamental frequency ($\omega^* = \theta_s^2 \omega$ for $\theta_s < 1$ and $\omega^* = \omega$ for $\theta_s > 1$) vs the simplified-flatness parameter θ_s for imperfect, angle-ply, simply supported, square cylindrical panels. The number of layers N_L is infinite, the imperfection wavenumbers are $j = k = 1$, and the fiber angle is $\theta = 15$ and 75 deg. Note that the fiber angle is measured from the axial direction. The frequency curves for 15 and 75 deg coincide for the perfect ($\mu = 0$) laminated cylindrical panels. The presence of a geometric imperfection will provide curvatures in the axial and circumferential directions and hence, they have two effects on the fundamental frequencies. First, regardless of the sign of the imperfection amplitude μ, the imperfection will provide a curvature in the axial direction, causing a significant increase in the fundamental frequencies. Second, since the perfect cylindrical panel has an outward curvature $1/R$ in the circumferential direction, a positive (bulge outwards as viewed from the origin) imperfection amplitude will increase the curvature further, whereas a negative (bulge inwards) imperfection amplitude will reduce it. Such reduction of the curvatures and hence the reduction of the frequencies (see the curves for $\mu = -1$) is more pronounced for the 75 deg than the 15 deg designs since the fiber lies predominantly in the circumferential direction (75 deg). Likewise, the increased frequency due to positive imperfection amplitude ($\mu = 1$) is also more pronounced for the 75 deg than the 15 deg configurations for the same reason. For a fixed value of the imperfection amplitude, the plotted fundamental frequencies are approximately constant for $\theta_s < 1$, indicating that the dimensional frequency is proportional to the square of the simplified-flatness parameter for $\theta_s < 1$.

Figure 2b shows a similar plot for the fiber angle $\theta = 45$ deg. Again, the fundamental frequencies for positive imperfection amplitudes are higher than those for the negative imperfections. At least for $\theta_s < 1$, the increase in the frequencies due to imperfection for $\theta = 45$ deg is less pronounced than that for the 15 or 75 deg designs, indicating that the 45 deg design may not always result in the largest fundamental frequency for an imperfect system.

In order to assess the sensitivity of the fundamental frequencies to various magnitudes of the imperfection amplitude, an appropriate graph is presented in Fig. 3a for simplified flatness parameter $\theta_s = 1$, fiber angle $\theta =$ (0 deg, 90 deg), (15 deg, 75 deg), and (45 deg) and number of layers $N_L = 2$ or infinite. For a positive imperfection amplitude, the increase in the fundamental frequencies is more pronounced for the 90 deg than the 0 deg configurations. Likewise, for a negative imperfection amplitude, the reduction in frequencies is more pronounced for the 90 deg than the 0 deg designs. Similar observations can be made by comparing the 15 and 75 deg curves. The $\theta = 45$ deg configuration is relatively insensitive to the presence of geometric imperfection. The frequencies actually lie below that for the $\theta = 15$ or 75 deg designs when the magnitude of the imperfection amplitude is approximately 0.9. Thus, the 45 deg design may not always yield the largest fundamental frequency for an imperfect angle-ply cylindrical panel. Comparing the $N_L = 2$ and $N_L =$ infinite curves, the reduction of the fundamental frequencies due to bending-stretching coupling (nonzero b^*_{ij}) is more pronounced for the 45 deg than the 75 deg designs.

Figure 3b shows a graph of the fundamental frequency vs fiber angle for imperfect, simply supported, angle-ply, square cylindrical panels. For the perfect system, the largest fundamental frequency occurs at $\theta = 45$ deg for $N_L =$ infinite, and at $\theta = 0$ deg for $N_L = 2$. However, for imperfect systems with imperfection amplitude $\mu = 1$ or $\mu = -1$ and $N_L = 2$ or infinite, the largest fundamental frequency occurs at fiber angle $\theta = 0$ deg, indicating that the $\theta = 45$ deg design does not always yield the largest fundamental frequency.

Figure 4a shows a plot of the fundamental frequency vs the normalized uniaxial axial compressive preload for imperfect, angle-ply, simply supported, square cylindrical panels, with simplified flatness parameter $\theta_s = 1$ and fiber angle $\theta = 0$ and 90 deg. The axial buckling load of a cylindrical panel with $\theta = \mu = 0$, $N_L =$ infinite is used as the normalizing factor

$$N_{x_c}(\theta = \mu = 0,\ N_L = \text{infinite}) = 35.8644(E_2 h^2/R) \tag{26}$$

Since the 90 deg configuration is weaker in the axial than the circumferential direction, the fundamental frequencies may correspond to higher values of m than unity. This causes a reduction in the frequencies (compared with the 0 deg design) for sufficiently large axial compressive preload. In fact, the fundamental frequencies for imperfect cylindrical panels with 0 deg rise with the axial preload, whereas they generally drop in the interaction curves for the 90 deg design.

Similar observations can be made by comparing the 15 and 75 deg designs plotted in Fig. 4b. Severe reductions in the fundamental frequencies due to bending-stretching coupling (nonzero b^*_{ij}) are found by comparing the $N_L = 2$ and $N_L =$ infinite interaction curves. Such reductions are especially pronounced for the $\theta = 45$ deg configurations, as shown in Fig. 4c.

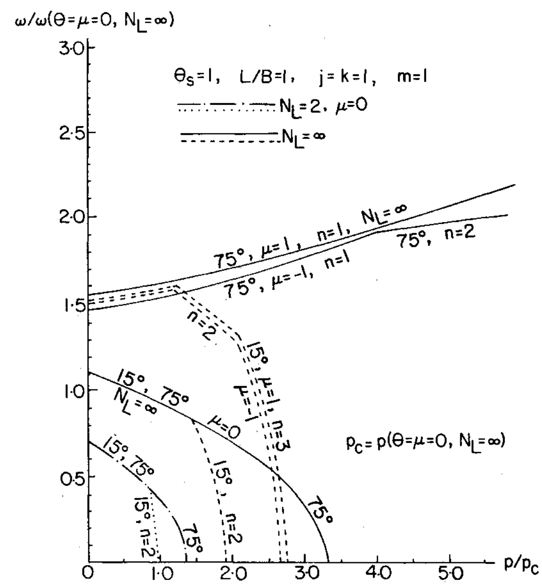

Fig. 5b Fundamental frequency vs external lateral pressure for imperfect angle-ply, simply supported, square cylindrical panels with $\theta_s = 1$ and fiber angle $\theta = 15$ and 75 deg.

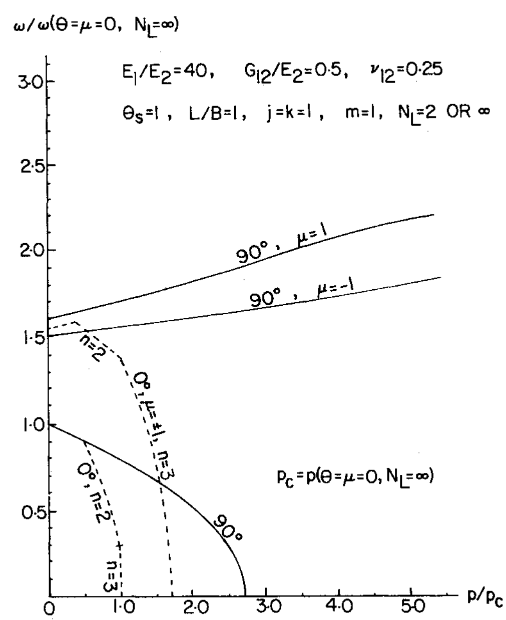

Fig. 5a Fundamental frequency vs external lateral pressure for imperfect angle-ply, simply supported, square cylindrical panels with $\theta_s = 1$ and fiber angle $\theta = 0$ and 90 deg.

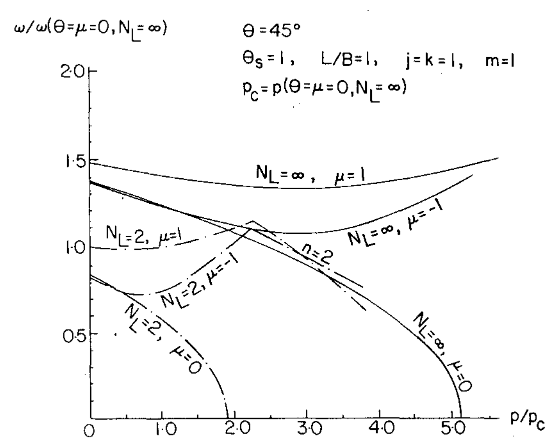

Fig. 5c Fundamental frequency vs external lateral pressure for imperfect angle-ply, simply supported, square cylindrical panels with $\theta_s = 1$ and fiber angle $\theta = 45$ deg.

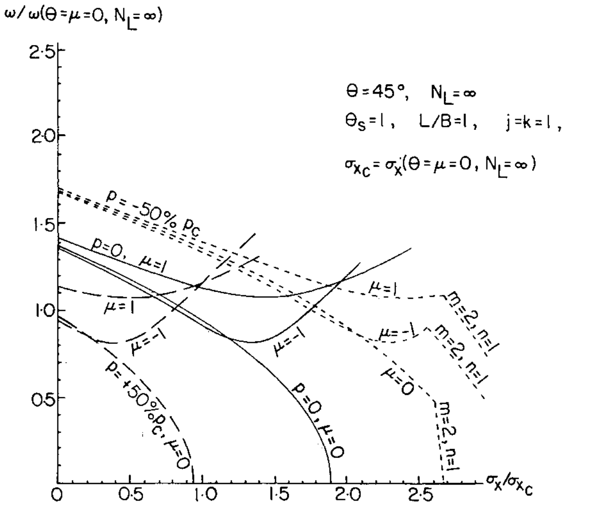

Fig. 6 Fundamental frequency vs axial compressive preload with external or internal pressure for imperfect angle-ply, simply supported, square cylindrical panels with $\theta_s = 1$ and fiber angle $\theta = 45$ deg.

Figure 5a depicts a plot of the fundamental frequency vs the normalized preload due to the external lateral pressure for imperfect angle-ply cylindrical panels with simplified-flatness parameter $\theta_s = 1$ and fiber angle $\theta = 0$ and 90 deg. The buckling load due to external lateral pressure for $\theta = \mu = 0$ and $N_L =$ finite is used as the normalizing factor

$$\bar{p}_c(\theta = \mu = 0,\ N_L = \text{infinite}) = 13.132(E_2 h^2/R^2) \qquad (27)$$

The fundamental frequencies for the 90 deg design in the presence of external pressurized preload are found to be much higher than that for the 0 deg designs. This is a situation quite opposite to that found in Fig. 4a for axial compressive preload. This indicates that a larger fiber angle ($\theta = 90$ deg, 75 deg) would result in a stiffer panel than the $\theta = 0$ deg, 15 deg designs, especially in the presence of geometric imperfections, as shown in Fig. 5b. The significant reductions of the fundamental frequencies for $\theta = 45$ deg due to bending-stretching coupling are shown in Fig. 5c. Comparing Figs. 5a-5c, the largest fundamental frequencies for the fiber angle $\theta = 45$ deg are generally lower than those for the other fiber orientations for imperfect systems.

Finally, a graph of the fundamental frequency vs the normalized axial compressive preload for imperfect angle-ply ($\theta = 45$ deg and $N_L =$ infinite) pressurized cylindrical panels is depicted in Fig. 6. The applied external (positive) and internal (negative) lateral pressures are chosen to be 50% of the lateral pressure needed to buckle the orthotropic shell for $\theta = \mu = 0$, $N_L =$ infinite. External pressure lowers the fundamental frequencies while internal pressure raises them. The curves for combined (axial compression and lateral pressure) preload and uniaxial preload behave similarly in a qualitative sense to each other. Thus, the results presented in this paper are likely to be qualitatively unchanged in the presence of an additional (at least, relatively small) lateral pressure.

V. Concluding Remarks

The effects of geometric imperfections on frequency-load interaction at angle-ply, square cylindrical panels simply supported along all four edges have been examined. The panel is subjected to the possibility of both axial compressive as well as internal or external lateral pressure preloads. The fundamental frequencies are found to be quite sensitive to the presence of small initial geometric imperfections and preloads. Particular attention is drawn to the effects of the sign of the imperfection amplitude, which causes a possible increase or decrease of the fundamental frequencies as well as a change in the optimum fiber angle and optimum wavenumbers of the fundamental mode. The $\theta = 45$ deg configuration may not always result in the largest fundamental frequency when compared with designs involving other fiber orientations. The work on vibrations of axially imperfect oval cylindrical shells was published as a separate paper.[19]

Acknowledgments

The authors are grateful for the financial support provided by The Ohio State University Seed Grant through the Office of Research and Graduate Studies. The generous use of the ADML and IRCC computer facilities is also acknowledged with thanks.

References

[1]Celep, Z., "Shear and Rotatory Inertia Effects on the Large Amplitude Vibration of the Initially Imperfect Plates," *Journal of Applied Mechanics*, ASME, Vol. 47, No. 3, Sept. 1980, pp. 662-666.

[2]Hui, D. and Leissa, A. W., "Effects of Geometric Imperfections on Vibrations of Biaxially Compressed Rectangular Flat Plates," *Journal of Applied Mechanics*, ASME, Vol. 50, No. 4, Dec. 1983, pp. 750-756.

[3]Ilanko, S., "Vibration Behaviour of In-Plane Loaded Thin Rectangular Plates with Initial Geometrical Imperfections," Ph.D. Thesis, Univ. of Western Ontario, Canada, Nov. 1985.

[4]Hui, D., "Influence of Geometric Imperfections and In-Plane Constraints on Nonlinear Vibrations of Simply Supported Cylindrical Panels," *Journal of Applied Mechanics*, ASME, Vol. 51, No. 2, June 1984, pp. 383-390.

[5]Rosen, A. and Singer, J., "Influence of Asymmetric Imperfections on Vibrations of Axially Compressed Cylindrical Shells," *Israel Journal of Technology*, Vol. 14, 1976, pp. 23-36; also TAE Rept. 212.

[6]Singer, J. and Prucz, J., "Influence of Initial Geometrical Imperfections on Vibrations of Axially Compressed Stiffened Cylindrical Shells," *Journal of Sound and Vibration*, Vol. 80, No. 1, 1982, pp. 117-143; (also TAE Rept. 369).

[7]Koval'chuk, P. S. and Krasnopol'skaya, T. S., "Resonance Phenomena in Nonlinear Vibrations of Cylindrical Shells with Initial Imperfections," *Soviet Applied Mechanics*, March 1980, pp. 867-872 (translated from *Prikladnaya Mekhanika*, Vol. 15, No. 9, 1979, pp. 100-107).

[8]Watawala, L. and Nash, W. A., "Influence of Initial Geometric Imperfections on Vibrations of Thin Circular Cylindrical Shells," *Computers and Structures*, Vol. 16, No. 1-4, 1983, pp. 125-130.

[9]Hui, D. and Leissa, A. W., "Effects of Uni-Directional Geometric Imperfections on Vibrations of Pressurized Shallow Spherical Shells," *International Journal of Nonlinear Mechanics*, Vol. 18, No. 4, 1983, pp. 279-285.

[10]Hui, D., "Effects of Geometric Imperfections on Frequency-Load Interaction of Biaxially Compressed Antisymmetric Angle Ply Rectangular Plates," *Journal of Applied Mechanics*, ASME, Vol. 52, No. 1, March 1985, pp. 155-162.

[11]Hui, D., "Soft-Spring Nonlinear Vibrations of Antisymmetrically Laminated Rectangular Plates," *International Journal of Mechanical Sciences*, Vol. 27, No. 6, June 1985, pp. 347-422.

[12]Kapania, R. and Yang, T., "Buckling, Postbuckling, and Nonlinear Vibrations of Imperfect Laminated Plates," *Nonlinear Analysis and NDE of Composite Material Vessels and Components*, edited by D. Hui, J. C. Duke, and H. Chung, ASME PVP-119-NDE-3, Chicago, July 1986, pp. 13-21.

[13]Bhattacharya, A. P., "Large Amplitude Vibrations of Imperfect Cross-Ply Laminated Cylindrical Shell Panels with Elastically Restrained Edges and Resting on Elastic Foundation," *Fibre Science and Technology*, Vol. 21, 1984, pp. 205-221.

[14]Hutchinson, J. W., "Axial Buckling of Pressurized Imperfect Cylindrical Shells," *AIAA Journal*, Vol. 3, Aug. 1986, pp. 1461–1466.

[15]Budiansky, B. and Amazigo, J. C., "Initial Post-Buckling Behavior of Cylindrical Shells under External Pressure," *Journal of Mathematics and Physics*, Vol. 47, 1968, pp. 223–235.

[16]Tennyson, R. C., Muggeridge, D. B., Chan, K. H., and Khot, N. S., "Buckling of Fiber-Reinforced Circular Cylinders under Axial Compression," AFFDL TR-72-102, Aug. 1972.

[17]Stephens, W., "Imperfection Sensitivity of Axially Compressed Stringer Reinforced Cylindrical Panels under Internal Pressure," *AIAA Journal*, Vol. 9, Sept. 1971, pp. 1713–1719.

[18]Soldatos, K. P., "Free Vibrations of Antisymmetric Angle-Ply Laminated Circular Cylindrical Panels," *Quarterly Journal of Mechanics and Applied Mathematics*, Vol. 36, Part 2, May 1983, pp. 207–221.

[19]Hui, D. and Du, I. H. Y., "Effects of Axial Imperfection on Vibrations of Anti-Symmetric Cross-Ply Oval Cylindrical Shells," *ASME Journal of Applied Mechanics*, Vol. 53, No. 3, Sept. 1986, pp. 675–680; also *Proceedings of 10th U.S. National Congress of Applied Mechanics*, Univ. of Texas at Austin, June 1986.

From the AIAA Progress in Astronautics and Aeronautics Series . . .

GASDYNAMICS OF DETONATIONS AND EXPLOSIONS—v. 75
and
COMBUSTION IN REACTIVE SYSTEMS—v. 76

Edited by J. Ray Bowen, University of Wisconsin,
N. Manson, Université de Poitiers,
A. K. Oppenheim, University of California,
and R. I. Soloukhin, BSSR Academy of Sciences

The papers in Volumes 75 and 76 of this Series comprise, on a selective basis, the revised and edited manuscripts of the presentations made at the 7th International Colloquium on Gasdynamics of Explosions and Reactive Systems, held in Göttingen, Germany, in August 1979. In the general field of combustion and flames, the phenomena of explosions and detonations involve some of the most complex processes ever to challenge the combustion scientist or gasdynamicist, simply for the reason that *both* gasdynamics and chemical reaction kinetics occur in an interactive manner in a very short time.

It has been only in the past two decades or so that research in the field of explosion phenomena has made substantial progress, largely due to advances in fast-response solid-state instrumentation for diagnostic experimentation and high-capacity electronic digital computers for carrying out complex theoretical studies. As the pace of such explosion research quickened, it became evident to research scientists on a broad international scale that it would be desirable to hold a regular series of international conferences devoted specifically to this aspect of combustion science (which might equally be called a special aspect of fluid-mechanical science). As the series continued to develop over the years, the topics included such special phenomena as liquid- and solid-phase explosions, initiation and ignition, nonequilibrium processes, turbulence effects, propagation of explosive waves, the detailed gasdynamic structure of detonation waves, and so on. These topics, as well as others, are included in the present two volumes. Volume 75, *Gasdynamics of Detonations and Explosions,* covers wall and confinement effects, liquid- and solid-phase phenomena, and cellular structure of detonations; Volume 76, *Combustion in Reactive Systems*, covers nonequilibrium processes, ignition, turbulence, propagation phenomena, and detailed kinetic modeling. The two volumes are recommended to the attention not only of combustion scientists in general but also to those concerned with the evolving interdisciplinary field of reactive gasdynamics.

Published in 1981, Volume 75—446 pp., 6×9, illus., $35.00 Mem., $55.00 List
Volume 76—656 pp., 6×9, illus., $35.00 Mem., $55.00 List

TO ORDER WRITE: Publications Dept., AIAA, 1633 Broadway, New York, N.Y. 10019